The role of the cleavage site 2′-hydroxyl in the *Tetrahymena* group I ribozyme reaction

Aiichiro Yoshida[1]*, Shu-ou Shan[2]*, Daniel Herschlag[2] and Joseph A Piccirilli[1]

Background: The 2′-hydroxyl of U preceding the cleavage site, U(–1), in the *Tetrahymena* ribozyme reaction contributes 10^3-fold to catalysis relative to a 2′-hydrogen atom. Previously proposed models for the catalytic role of this 2′-OH involve coordination of a catalytic metal ion and hydrogen-bond donation to the 3′-bridging oxygen. An additional model, hydrogen-bond donation by the 2′-OH to a nonbridging reactive phosphoryl oxygen, is also consistent with previous results. We have tested these models using atomic-level substrate modifications and kinetic and thermodynamic analyses.

Results: Replacing the 2′-OH with -NH_3^+ increases the reaction rate ~60-fold, despite the absence of lone-pair electrons on the 2′-NH_3^+ group to coordinate a metal ion. Binding and reaction of a modified oligonucleotide substrate with 2′-NH_2 at U(–1) are unaffected by soft-metal ions. These results suggest that the 2′-OH of U(–1) does not interact with a metal ion. The contribution of the 2′-moiety of U(–1) is unperturbed by thio substitution at either of the nonbridging oxygens of the reactive phosphoryl group, providing no indication of a hydrogen bond between the 2′-OH and the nonbridging phosphoryl oxygens. In contrast, the 10^3-fold catalytic advantage of 2′-OH relative to 2′-H is eliminated when the 3′-bridging oxygen is replaced by sulfur. As sulfur is a weaker hydrogen-bond acceptor than oxygen, this effect suggests a hydrogen-bonding interaction between the 2′-OH and the 3′-bridging oxygen.

Conclusions: These results provide the first experimental support for the model in which the 2′-OH of U(–1) donates a hydrogen bond to the neighboring 3′-bridging oxygen, thereby stabilizing the developing negative charge on the 3′-oxygen in the transition state.

Addresses: [1]Departments of Biochemistry and Molecular Biology, and Chemistry, University of Chicago, 5841 S. Maryland Avenue, MC1028, Chicago, IL 60637, USA. [2]Department of Biochemistry, B400 Beckman Center, Stanford University, Stanford, CA 94305-5307, USA.

Correspondence: Daniel Herschlag; Joseph A Piccirilli
E-mail: herschla@cmgm.stanford.edu; jpicciri@midway.uchicago.edu

*These authors contributed equally to this work.

Key words: chemical modification, mechanistic analysis, RNA catalysis

Received: **16 August 1999**
Revisions requested: **22 September 1999**
Revisions received: **7 October 1999**
Accepted: **18 October 1999**

Published: **11 January 2000**

Chemistry & Biology 2000, **7**:85–96

1074-5521/00/$ – see front matter

Introduction

The *Tetrahymena* ribozyme (E) derived from a self-splicing group I intron catalyzes a transesterification reaction:

$$\mathrm{CCC}\underset{(S)}{\mathrm{U}}\mathrm{CU_pA} + \mathrm{G_{OH}} \rightarrow \mathrm{CCC}\underset{(P)}{\mathrm{U}}\mathrm{CU_{OH}} + \mathrm{G_pA} \quad (1)$$

in which an exogenous guanosine nucleophile (G) cleaves a specific phosphodiester bond of an oligonucleotide substrate (S; Table 1; see [1] and references therein). The 2′-OH of U preceding the scissile bond [U(–1)] facilitates the chemical step ~10^3-fold relative to 2′-H, but does not affect binding of S [2]. This corresponds to a contribution of ~4 kcal/mol specifically to transition-state stabilization. Linear free energy analysis with oligonucleotide substrates bearing a series of 2′-substituents at U(–1) suggested that the rate effect of the 2′-OH is more than that expected from simple inductive effects [2]. Specific interactions of the 2′-OH may therefore contribute to catalysis.

How does this 2′-OH facilitate the reaction? Three models can be postulated that are consistent with results from previous biochemical studies and reasonable from geometric and chemical considerations: first, the 2′-OH interacts with an active-site metal ion that is crucial for catalysis (Figure 1a); second, the 2′-OH donates a hydrogen bond to the 3′-bridging oxygen (Figure 1b); and third, the 2′-OH donates a hydrogen bond to one of the nonbridging oxygens of the reactive phosphoryl group (Figure 1c). The first two models have been much discussed (Figure 1a,b; see below) [2–7], whereas the interaction with the reactive phosphoryl oxygen (Figure 1c) has not been considered previously. Nevertheless, the interactions postulated in these models have yet to be tested directly.

A metal-ion interaction with the 2′-OH (Figure 1a) was initially proposed on the basis of the observation that reaction of a CU (or CT) dinucleotide with a circular form of the *Tetrahymena* intron has different Mg^{2+} concentration dependencies with 2′-OH and 2′-H at U(–1) [3,8]. Similar observations and proposals have been made with the RNA component of RNase P [9]. In addition, the 2′-OH of the guanosine nucleophile interacts with an active-site metal

Table 1

List of oligonucleotide substrates.

	Abbreviation	Oligonucleotide substrate									
			−5		−3		−1 +1		+3		+5
I	rS_{OH}	rC	rC	rC	rU	rC	rU-OpO-rA	rA	rA	rA	rA
II	rS_{H}	rC	rC	rC	rU	rC	dT-OpO-rA	rA	rA	rA	rA
III	rS_{N}	rC	rC	rC	rU	rC	nU-OpO-rA				
IV	dS_{OH}	dC	dC	dC	dU	dC	rU-OpO-dA	dA	dA	dA	dA
V	dS_{H}	dC	dC	dC	dU	dC	dT-OpO-dA	dA	dA	dA	dA
VI	dS_{N}	dC	dC	dC	dU	dC	nU-OpO-dA	dA	dA	dA	dA
VII	$rS_{OH,3'-S}$	mC	mC	mC	rU	rC	rU-SpO-rA				
VIII	$rS_{H,3'-S}$	mC	mC	mC	rU	rC	dU-SpO-rA				
IX	$rS_{OH,P-S}$	mC	mC	mC	rU	rC	rU-OpS-rA				
X	$rS_{H,P-S}$	mC	mC	mC	rU	rC	dU-OpS-rA				
XI	$rS_{N,P-S}$	rC	rC	rC	rU	rC	nU-OpS-rA				

S refers to the oligonucleotide substrate $CCCUCUA_5$ or CCCUCUA, without specification of the sugar identity. The presence of additional A residues at the (+2) to (+5) position of S does not affect binding or the reaction rate (R. Russell & D.H., unpublished observations). r refers to 2′-OH; d refers to 2′-H; m refers to 2′-OCH_3; n refers to 2′-amino, without specification of the protonation state. In the text, $rSNH_3^+$ and $rSNH_2$ refer to the oligonucleotide rS_N with the 2′-amino group protonated and deprotonated, respectively. 3'-S refers to the presence of a thio substitution at the 3′-bridging oxygen of U(−1); P-S refers to the presence of a thio substitution at the *pro*-S_P oxygen of the reactive phosphoryl group. 2′-OCH_3 groups were introduced into the (−4) to (−6) residues of 3′-S or P-S containing substrates; the sole effect of this modification is to prevent miscleavage of these substrates, allowing more accurate determination of reaction rates [28,59]. The chemical composition of the reactive phosphoryl group is specified as follows:

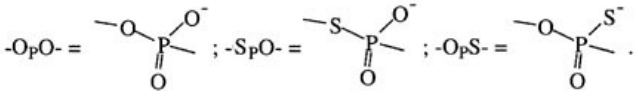

ion (Figure 1, M_C) [7,10], rendering an analogous metal-ion interaction with the 2′-OH of U(−1) an appealing model. There are multiple metal ions within the active site of the *Tetrahymena* ribozyme (Figure 1, M_A, M_B and M_C) [7,11–14]. The 2′-OH could, with reasonable geometry, coordinate the metal ion interacting with the 3′-bridging oxygen (Figure 1a, M_A) [11], a metal ion interacting with the *pro*-S_P oxygen of the reactive phosphoryl group [14], or an unidentified active-site metal ion. The previous experimental results [3,8] do not distinguish, however, between direct coordination of a metal ion by this 2′-OH or indirect contribution of this 2′-OH to Mg^{2+} binding through intervening active-site groups, nor is it known whether the same reaction steps were followed with the substrates bearing a 2′-OH and 2′-H.

A hydrogen bond between the 2′-OH and the 3′-bridging oxygen (Figure 1b) was subsequently proposed [2]. The

Figure 1

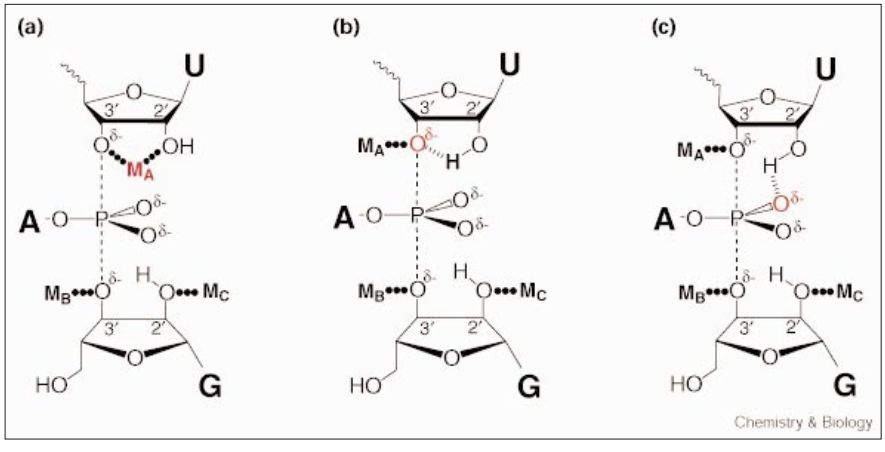

Models for the catalytic role of the 2′-OH of U(−1) within the *Tetrahymena* group I ribozyme active site. The large bold letters represent nucleotide bases on the oligonucleotide substrate and the guanosine nucleophile, the dashed lines (---) depict the partial bond from the reactive phosphorus to the 3′-OH of G and the 3′-oxygen of the U(−1) residue of S, and 'δ-' depicts the partial negative charges on the 3′-oxygens of U(−1), the 3′-oxygen of G, and the nonbridging oxygens of the reactive phosphoryl group in the reaction's transition state. M_A is the metal ion interacting with the 3′-bridging oxygen of U (−1) [11], M_B is the metal ion interacting with the 3′-moiety of G [12], and M_C is the metal ion interacting with the 2′-moiety of G [7,10]. **(a)** The 2′-OH of U(−1) interacts with a catalytic metal ion. An interaction with M_A is depicted as an example of potential metal ion interaction(s) with this 2′-OH; an alternative interaction with another active-site metal ion is also possible. **(b)** The 2′-OH donates a hydrogen bond to the neighboring 3′-bridging oxygen. **(c)** The 2′-OH donates a hydrogen bond to one of the nonbridging oxygens of the reactive phosphoryl group.

rate of the chemical step for the substrate with 2′-OH is ~tenfold faster than that for the substrate with a 2′-fluoro group at U(–1), despite the weaker electron-withdrawing ability of 2′-OH than 2′-F [2]. As a 2′-fluoro group contains lone-pair electrons that can accept hydrogen bonds but cannot donate hydrogen bonds, the higher reactivity of the substrate with 2′-OH than 2′-F at U(–1) suggests that hydrogen-bond donation from the 2′-OH of U(–1) might be important. A hydrogen bond from this 2′-OH to the neighboring 3′-oxygen is the simplest model that accounts for the specific transition-state stabilization provided by the 2′-OH, as negative charge develops on the 3′-bridging oxygen in the course of the reaction and could be stabilized by such a hydrogen bond [2,15–17]. This model has been widely accepted, and extensions of this model have been proposed (see below). Nevertheless, the model has not been tested. Even if the 2′-OH of U(–1) acts as a hydrogen-bond donor, the hydrogen bond could alternatively be donated to one of the nonbridging oxygens of the reactive phosphoryl group, which may develop additional negative charge in the transition state (Figure 1c). To our knowledge, this interaction has not been discussed previously but is reasonable from geometrical considerations and is consistent with all of the previous data.

Besides the interactions depicted in the models shown in Figure 1, additional active-site interactions with the 2′-OH of U(–1) have been suggested. The rate advantage provided by this 2′-OH relative to 2′-H is reduced ~fivefold when the G•U wobble pair is replaced by a G•C pair [4], and ≥ 30-fold when the 2′-OH of A207 is replaced by a 2′-H or 2′-F [6]. A crystal structure of an RNA duplex containing a G•U pair revealed an ordered water molecule bridging the 2′-OH of U and the exocyclic amine of G [18,19]. The biochemical data, in conjunction with the crystallographic observations, led to the proposal of a hydrogen-bonding network in which a hydroxyl group, later identified as the 2′-OH of A207, donates a hydrogen bond to the 2′-OH of U(–1) and accepts a hydrogen bond from the exocyclic amine of G22, thereby bridging the cleavage site 2′-OH and the G•U wobble pair [4,6,18]. Building on the earlier proposal [2], this network was suggested to orient the 2′-OH of U(–1) to favor its interaction with the 3′-bridging oxygen (Figure 1b) [4,6]. Nevertheless, the results of these studies are also consistent with the other models: the 2′-OH could alternatively be aligned to interact with one of the nonbridging phosphoryl oxygens (Figure 1c), or one of the lone-pair electrons of this 2′-OH could accept a hydrogen bond from A207, while the other electron pair interacts with an active-site metal ion (Figure 1a).

In this work, each of the catalytic models depicted in Figure 1 has been tested by atomic-level modifications of the substrate combined with quantitative kinetic and thermodynamic analysis. The results provide no indication of a metal-ion interaction with the 2′-OH or a hydrogen bond between this 2′-OH and a nonbridging reactive phosphoryl oxygen. In contrast, the results support the model of Figure 1b, in which the 2′-OH of U(–1) donates a hydrogen bond to the 3′-bridging oxygen.

Results and discussion

We first describe experiments that test for metal-ion interactions with the 2′-OH of U(–1) (Figure 1a). Two independent approaches were used: replacing the 2′-OH with 2′-NH_3^+ and investigating its effect on reactivity; and replacing the 2′-OH with 2′-NH_2 and exploiting the preference of the -NH_2 group to interact with metal ions softer than Mg^{2+}. The next section describes experiments that test hydrogen-bonding interactions of the 2′-OH with the nonbridging reactive phosphoryl oxygens and with the 3′-bridging oxygen (Figure 1b and c, respectively). These experiments support a hydrogen bond between the 2′-OH and the 3′-bridging oxygen (Figure 1b) and suggest that the other proposed interactions are not made (Figure 1a,c).

A metal-ion interaction with the 2′-OH of U(–1)?

To test whether a metal-ion interaction with the 2′-OH of U(–1) is important for catalysis (Figure 1a), we investigated the reactivity of the oligonucleotide substrate $rS^{NH_3^+}$, in which the 2′-OH is replaced by -NH_3^+ (Table 1). The –NH_3^+ group has no lone pair electrons and therefore cannot interact with a metal ion. The $rS^{NH_3^+}$ reaction would therefore be expected to be severely compromised if the 2′-OH coordinates a metal ion important for catalysis (e.g. [10]).

To determine the reactivity of $rS^{NH_3^+}$, it was necessary to establish the reaction conditions under which the 2′-amino group of rS_N (Table 1) is protonated and under which the chemical step is rate limiting. We therefore first determined the effect of pH on the reaction of rS_N and probed whether the chemical step is rate limiting, as described below. The pH dependence of the rS_N reaction could then be compared with those of rS_{OH} and rS_H to determine the effect of the 2′-NH_3^+ substitution on reactivity.

To follow the reaction of protonated $rS^{NH_3^+}$, a pH value below the pK_a of the 2′-amino group must be used. (A 2′-NH_3^+ group deprotonates with a pK_a of ~6.2 in aqueous solution [20]; the pK_a of this group is even lower with rS_N bound to the ribozyme, as described below.) Preliminary experiments indicated that ribozyme activity is severely compromised below pH 5 with the standard Mg^{2+} concentration of 10 mM, possibly due to disruption of ribozyme structure at low pH ([21]; D.S. Knitt and D.H., unpublished results). This deleterious effect of low pH can be overcome at Mg^{2+} concentrations above 50 mM, as expected from stabilization of the active ribozyme structure by Mg^{2+} [22–24]. A Mg^{2+} concentration of 100 mM was therefore used in the following experiments.

Table 2

Nomenclature for rate constants.

Rate constant	Reaction
k_c^G	E•S•G → products
$(k_c / K_m)^G$	E•S + G → products
$(k_c/K_m)^S$	E•G + S → products

The rate of the reaction E•rS_N + G → products [$(k_c/K_m)^G$; Table 2] was determined as a function of pH (Figure 2a, filled circles). $(k_c/K_m)^G$ for rS_N increases with increasing pH below pH 5.0 but begins to level off at higher pH. To isolate the effect that arises specifically from deprotonation of the $-NH_3^+$ group, the pH dependence for the reaction of the wild-type substrate rS_{OH} was determined in parallel. As observed previously at 10 mM Mg^{2+} [25], $(k_c/K_m)^G$ for rS_{OH} increases log-linearly with pH below pH 7.1 but levels off at higher pH (Figure 2a, open circles). Comparison of the pH dependencies for the rS_N and rS_{OH} reactions is complicated, however, as the apparent leveling off of $(k_c/K_m)^G$ for rS_{OH} at high pH results from a change in rate-limiting step from chemical cleavage to a conformational step ([25] and M. Khosla and D.H., unpublished observations). Indeed, $(k_c/K_m)^G$ for rS_H, for which the chemical step is ~10^3-fold slower than rS_{OH} and is rate limiting over the entire pH range [25,26], has a log-linear pH dependence up to pH 8.5 (Figure 2a, open squares). The apparent leveling off of $(k_c/K_m)^G$ for the rS_N reaction above pH 5.0 could arise from different reactivities of $rSNH_3^+$ and $rSNH_2$, a change in rate-limiting step analogous to the rS_{OH} reaction, or a combination of these effects.

To differentiate between these possibilities, we examined the effect of thio substitution at the *pro-*R_P oxygen of the reactive phosphoryl group on the observed reaction rate. The sole effect of this substitution is to slow down the rate of the chemical step 2–3-fold for reaction of this ribozyme, similar to effects observed with model compounds [25,27]. The thio modification slows the rate of

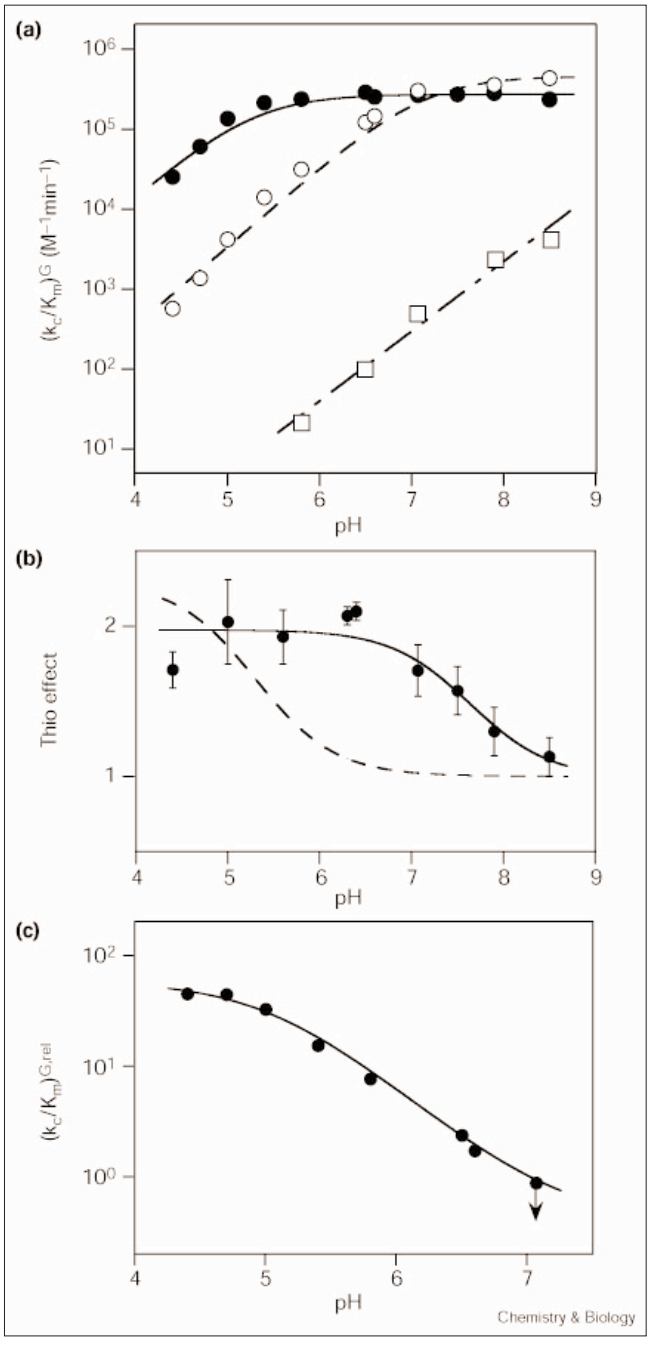

Figure 2

$rSNH_3^+$ is more reactive than rS_{OH}. **(a)** The pH dependencies of the rate constant of reaction E•S + G → products [$(k_c / K_m)^G$] with rS_N (●), rS_{OH} (○) and rS_H (□), determined as described in the Materials and methods section (100 mM Mg^{2+}). **(b)** The pH dependence of the effect of thio-substitution at the *pro-*R_P oxygen of the reactive phosphoryl group on $(k_c / K_m)^G$ for rS_N [thio effect = $(k_c / K_m)^G_{oxy}$ / $(k_c / K_m)^G_{thio}$]. The thio effect at each pH represents the average of at least two independent experiments, in which observed rate constants for substrates with and without thio substitution were determined side-by-side in triplicate ((a) and data not shown). The dotted line shows the predicted pH dependence of the thio effect if the rate-limiting step for the rS_N reaction above pH 5.0 changes to a step with a thio effect of 1. **(c)** The pH dependence of the reactivity of rS_N relative to rS_{OH} [$(k_c / K_m)^{G,rel} = (k_c / K_m)^G_{rS_N} / (k_c / K_m)^G_{rS_{OH}}$]. Values of $(k_c / K_m)^G$ for each substrate were from part (a). The line is a fit of the data to equation 3, derived from equation 2 in the Results and discussion section (see the Materials and methods section), and gives $(k_c / K_m)^{G,rel}_{rSNH_3^+} = 58 \pm 5$ and $pK_a^{E•rS_N} = 5.0 \pm 0.2$. The relative reactivity of $rSNH_2$, $(k_c / K_m)^{G,rel}_{rSNH_2}$, could not be determined, because the pH dependence of $(k_c / K_m)^{G,rel}$ would need to be extended above pH 7.1, whereas interpretation of $(k_c / K_m)^{G,rel}$ values above pH 7.1 is complicated by the change in rate-limiting step for the rS_N reaction suggested by the decreased thio effect ((b); see text). Values of $(k_c / K_m)^{G,rel}$ were therefore plotted only from pH 4.4 to 7.1. The arrow on the data point at pH 7.1 depicts that the observed $(k_c / K_m)^{G,rel}$ is an upper limit for the relative reactivity of rS_N in the chemical step. This is because the chemical step is rate limiting for $(k_c / K_m)^G$ of rS_N at pH 7.1, whereas there is a change in the rate-limiting step for $(k_c / K_m)^G$ of rS_{OH} at this pH, as described in the text.

the rS_N reaction by a constant amount, 1.9 ± 0.3-fold, from pH 4.4 to 6.6 (Figure 2b). If the apparent leveling off of $(k_c/K_m)^G$ for the rS_N reaction represented a change in the rate-limiting step, then the thio effect would be expected to decrease above pH 5.0 (Figure 2b, dashed line), where $(k_c/K_m)^G$ for rS_N levels off (Figure 2a). The thio effect therefore suggests that the chemical step is rate limiting for reaction of rS_N above pH 5.0. Above pH 7, the thio effect begins to decrease (Figure 2b), possibly reflecting a change in rate-limiting step for the rS_N reaction at the highest pH values, analogous to rS_{OH}. Reactions at these high pH values were therefore not analyzed here.

As the chemical step is rate limiting for both the rS_N and rS_{OH} reaction below pH 7.1, the effect on reactivity of rS_N that arises specifically from deprotonation of the $-NH_3^+$ group can be isolated by plotting the values of $(k_c/K_m)^G$ for rS_N relative to that for rS_{OH} as a function of pH [$(k_c/K_m)^{G,rel} = (k_c/K_m)^G_{rS_N} / (k_c/K_m)^G_{rS_{OH}}$; Figure 2c]. At the lowest pH values (4.4–4.7), rS_N reacts 44-fold faster than rS_{OH}. $(k_c/K_m)^{G,rel}$ decreases with increasing pH above pH 5.0 (Figure 2c), suggesting that $rSNH_2$ is less reactive than $rSNH_3^+$:

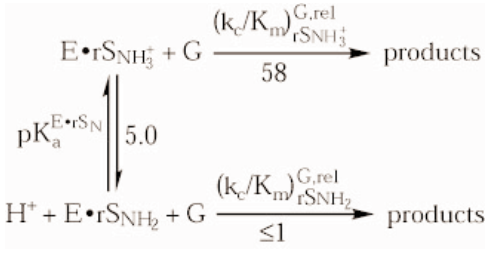

(2)

A fit of the pH dependence of $(k_c/K_m)^{G,rel}$ in Figure 2c to the model of equation 2 gives $(k_c/K_m)^{G,rel}_{rSNH_3^+} = 58 \pm 5$ for the reactivity of $rSNH_3^+$ relative to rS_{OH}, and $pK_a^{E•rS_N} = 5.0 \pm 0.2$ for deprotonation of the 2′-NH_3^+ group in the E•rS_N complex. This pK_a value is lower than the solution pK_a value of 6.2 for the 2′-amino group [20], presumably because of perturbation of the pK_a when rS_N is bound to the ribozyme (see the Materials and methods section and [20,28] for details). As $(k_c/K_m)^{G,rel}$ continues to decrease from pH 5.0 to 7.1, the reaction observed over this pH range arises from a small fraction of the more reactive species $rSNH_3^+$, whereas $rSNH_2$ makes a negligible contribution to the observed reaction rate.

The higher reactivity of $rSNH_3^+$ than rS_{OH}, despite the absence of lone-pair electrons on the 2′-NH_3^+ group to interact with a metal ion, suggests that a metal-ion interaction with the 2′-OH of U(–1) is not important for catalysis by the *Tetrahymena* ribozyme. An alternative model, in which a metal-ion interaction with the 2′-OH in the wild-type reaction is replaced by the positively charged $-NH_3^+$ group, remains possible but not likely, because replacing a catalytic interaction with a fortuitous interaction would not be expected to increase reactivity.

To probe independently for a metal ion coordinated by the 2′-moiety of U(–1), we examined the effect of soft-metal ions on the reactivity of the oligonucleotide substrate with a 2′-NH_2 group at U(–1). These experiments are based on the observation that nitrogen ligands typically prefer to interact with soft-metal ions than with Mg^{2+}, whereas oxygen ligands do not exhibit such preferences [10,29,30]. This approach has previously been used to identify a metal-ion interaction with the 2′-OH of the guanosine nucleophile in this ribozyme (Figure 1, M_C) [7,10]. Analogous metal-ion rescue of the reaction of modified oligonucleotide substrates with 2′-NH_2 at U(–1) might be expected if a metal-ion interaction with the 2′-moiety of G is crucial for catalysis.

To provide a most sensitive probe for a potential metal-ion interaction with the 2′-NH_2 of U(–1), the reaction E•G + S → products [$(k_c/K_m)^S$; Table 2] was followed. In this reaction, S is not bound to the ribozyme in the starting ground state, so that any interactions with active-site metal ions would be formed in the course of the reaction, allowing the observed reaction rate to provide a probe for such an interaction. To ensure that the chemical step was rate limiting, the oligonucleotide substrate dS_N (Table 1) was used. Replacing the 2′-OH groups of S with 2′-H at residues other than U(–1) weakens binding of S, but does not affect the rate of the chemical step once S is bound within the ribozyme active site [31]. The pH dependence of $(k_c/K_m)^S$ and additional observations strongly suggest that the chemical step is rate limiting for the dS_N reaction and, furthermore, that the reaction of $dSNH_2$ can be followed at pH 7.5, without significant contribution from reaction of the small fraction of $dSNH_3^+$ present at this pH (0.05; pK_a ~ 6.2 [20]; see the Materials and methods section).

The effect of soft-metal ions on the rate constant of the reaction E•G + $dSNH_2$ → products was determined in a background of 10 mM Mg^{2+}. Addition of Mn^{2+}, up to 10 mM, had the same effect on the reaction E•G + S → products with $dSNH_2$ as with dS_H (Figure 3a,b; 10 mM Mg^{2+}). Mn^{2+} does not, therefore, provide a specific stimulation of the reaction of $dSNH_2$ (relative to dS_H). Similarly, addition of several other soft-metal ions, Zn^{2+}, Cd^{2+} and Co^{2+}, did not provide a specific stimulation for reaction of $dSNH_2$ relative to dS_H at concentrations up to 0.5, 0.5 and 5 mM, respectively (data not shown).

To allow Mn^{2+} to compete more effectively with Mg^{2+} at the potential metal site, we lowered the concentration of Mg^{2+} to 0.1 mM and used even higher Mn^{2+} concentrations. Nevertheless, addition of up to 50 mM Mn^{2+} did not provide a specific stimulation for reaction of $dSNH_2$ relative to dS_H [Figure 3c,d; analogous results were

Figure 3

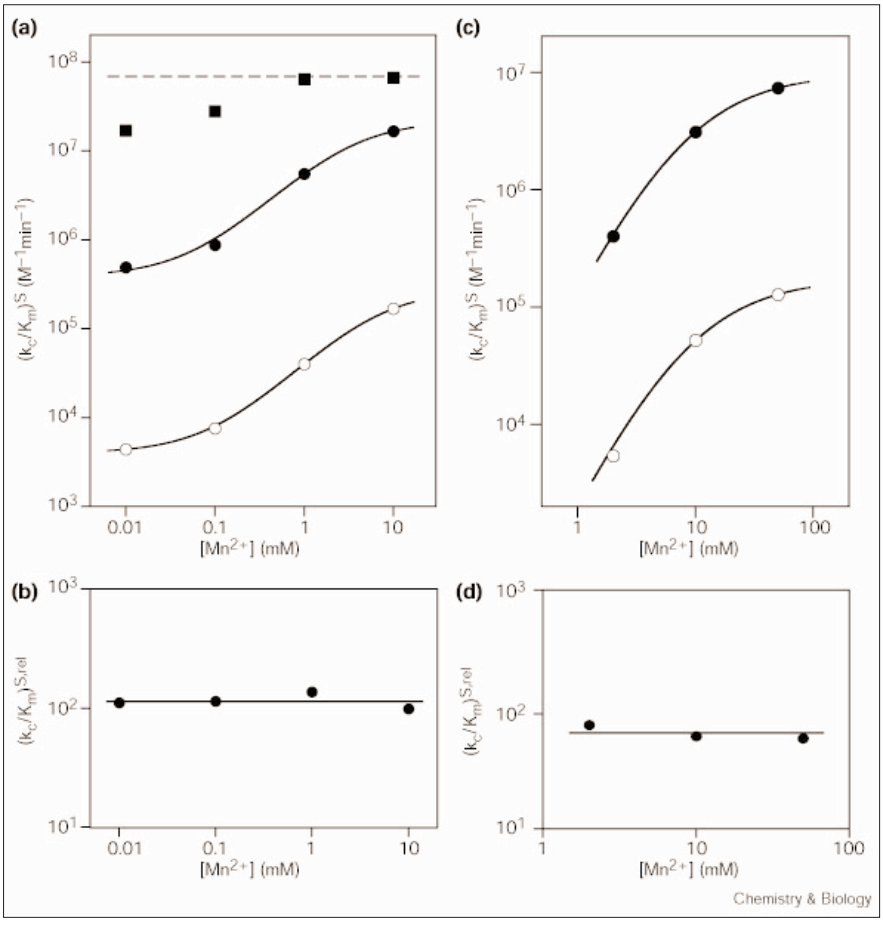

Mn^{2+} does not stimulate the reaction of dS_{NH_2}. **(a)** Effect of Mn^{2+} on the rate constant of the reaction E•G + S → products $[(k_c / K_m)^S]$ with dS_N (●), dS_{OH} (■) and dS_H (○). The second-order rate constant $(k_c / K_m)^S$ was determined at pH 7.5 with 10 mM Mg^{2+} background, as described in the Materials and methods section. The dashed line denotes that $(k_c / K_m)^S$ for dS_{OH} above 1 mM Mn^{2+} is limited by the binding of the substrate instead of the chemical step (S.S. and D.H., unpublished observations). **(b)** Effect of Mn^{2+} on the reactivity of dS_{NH_2} relative to dS_H in the reaction: E•G + S → products $[(k_c / K_m)^{S,rel} = (k_c / K_m)^S_{dS_N} / (k_c / K_m)^S_{dS_N}]$. Values of $(k_c / K_m)^S$ were from part (a). The straight line with a slope of zero denotes the absence of an effect of Mn^{2+} on $(k_c / K_m)^{S,rel}$. **(c)** Same as in (a) except that a background of 0.1 mM Mg^{2+} was used instead of 10 mM. **(d)** Same as in (b) except that a 0.1 mM Mg^{2+} background was used. Values of $(k_c / K_m)^S$ were from (c). The straight line with a slope of zero denotes the absence of an effect of Mn^{2+} on $(k_c / K_m)^{S,rel}$.

obtained in reactions with a background of 2 mM Mg^{2+} (data not shown)]. Thus, if a Mn^{2+} could interact with the 2′-NH_2 group more strongly than Mg^{2+} relative to 2′-OH, this Mn^{2+} would need to bind much more weakly than Mg^{2+} to this metal-ion site in the E•G complex. For example, if replacing the Mg^{2+} at the potential metal site with Mn^{2+} provides a tenfold stimulation for the dS_{NH_2} reaction relative to dS_H, then this metal site would bind Mg^{2+} 5000-fold more strongly than Mn^{2+} [Mg^{2+} specificity = ($[Mn^{2+}] / [Mg^{2+}]$) × rate enhancement = (50/0.1) × 10 = 5000]. An even greater Mg^{2+} specificity would be required if the rate enhancement provided by the potential Mn^{2+} ion were larger.

The absence of metal-ion rescue of the dS_{NH_2} reaction is in marked contrast to the ability of Mn^{2+} and Zn^{2+} to rescue the reaction of G_{NH_2}, in which the 2′-OH of G is replaced by -NH_2, in the *Tetrahymena* ribozyme and other group I ribozymes (20-fold and ≥ 60-fold rescue of the G_{NH_2} reaction by Mn^{2+} and Zn^{2+}, respectively) [7,10]. In solution, compounds containing nitrogen ligands typically interact 10–10^2-fold more strongly with Mn^{2+} and 10^2–10^3-fold more strongly with Zn^{2+}, Co^{2+} and Cd^{2+} than with Mg^{2+}, whereas compounds containing exclusively oxygen ligands do not typically exhibit such strong preferences [29,30]. Finally, substantially stronger binding of Mg^{2+} than Mn^{2+} to the potential metal-ion site is contrary to previous studies of metal-ion–RNA interactions, in which similar or stronger binding of Mn^{2+} than Mg^{2+} was observed (e.g. [10,32–34]). Although a metal-ion interaction with the 2′-OH cannot be ruled out on the basis of negative results, these results are most simply accounted for by the absence of a metal-ion interaction with the 2′-moiety of U(–1).

In summary, the higher reactivity of the substrate with a 2′-NH_3^+ group than a 2′-OH group at U(–1) and the absence of metal-ion rescue of reaction of the substrate with 2′-NH_2 suggest that the 2′-OH of U(–1) does not interact with an active-site metal ion. This and previous results [13] suggest an asymmetry in transition-state interactions at the *Tetrahymena* ribozyme active site, with a metal ion interacting with the 2′-OH of the guanosine nucleophile but not with the 2′-OH of U(–1). The absence of a metal-ion interaction with the 2′-OH of U(–1) also

provides an explanation for the substantially larger deleterious effect of removing the 2′-OH of the guanosine nucleophile than the 2′-OH of U(–1) (>10^6-fold compared with 10^3-fold reduction in the rate of the chemical step; [35,36], and S. S. and D.H., unpublished observations), as placing a hydrogen atom adjacent to a metal ion is likely to have major energetic consequences.

Hydrogen-bond donation from the 2′-OH of U(–1)?

The faster chemical step for oligonucleotide substrates with 2′-OH than with 2′-F at U(–1) suggested that hydrogen-bond donation from the 2′-OH of U(–1) contributes to catalysis (see above) [2]. As described in the Introduction section, however, there are three substrate atoms that could potentially accept a hydrogen bond from this 2′-OH: the neighboring 3′-bridging oxygen, or the *pro*-R_P or *pro*-S_P oxygen of the reactive phosphoryl group (Figure 1b and c, respectively). In this section, each of these potential hydrogen-bonding interactions was tested by replacing the oxygen with sulfur. As sulfur is a weaker hydrogen-bond acceptor than oxygen ([37–42] and references therein), thio substitution would be expected to diminish the catalytic advantage provided by a hydrogen bond from the 2′-OH.

Several previous observations suggest that there are no catalytically important active-site interactions with the *pro*-R_P oxygen of the reactive phosphoryl group. Thio substitution of the *pro*-R_P oxygen reduces the rate of the chemical step only 2–3-fold, consistent with the effects observed in reactions of model compounds ([25,27]; see also above). In addition, similar thio effects at the *pro*-R_P oxygen were observed with substrates containing 2′-OH or 2′-H at U(–1) ([25] and data not shown), suggesting that there is no interaction between the 2′-OH and the *pro*-R_P oxygen.

Thio substitution at the *pro*-S_P oxygen reduces the rate of the chemical step ~10^3-fold ([27] and see below), strongly suggesting the presence of active-site interactions with the *pro*-S_P oxygen (e.g. [14]). To probe a potential hydrogen bond between the *pro*-S_P oxygen and the 2′-OH of U(–1), the effect of thio substitution at this oxygen was investigated with substrates bearing a series of 2′-substituents (Table 1, substrates I–III compared with IX–XI). Reactions were carried out under conditions such that the chemical step is rate limiting for each substrate (Table 3). To facilitate accurate determination of rate constants, we used saturating ribozyme concentrations with respect to S, such that the reactions E•S + G → products and E•S•G → products

Table 3

Thio-effects at the *pro*-S_p oxygen of the reactive phosphoryl group with different 2′-substituents at U(–1).*

2′-X†	pH	$(k_c / K_m)^G$ ($M^{-1}min^{-1}$)		Thio effect§	pH	k_c^G (min^{-1})		Thio effect§
		P–O	P–S			P–O	P–S	
OH	5.5	1.3×10^4	2.0	6.5×10^3	4.4	0.13	6.5×10^{-5}	2.0×10^3
	6.2	1.1×10^5	17	6.5×10^3	4.4‡	0.29	1.9×10^{-4}	1.5×10^3
					5.0	0.45	4.6×10^{-4}	0.98×10^3
					5.0‡	1.05	9.1×10^{-4}	1.2×10^3
H		–	–	–	7.9	0.25	2.3×10^{-4}	1.1×10^3
					7.5	0.16	9.7×10^{-5}	1.6×10^3
					7.0	0.034	2.6×10^{-5}	1.3×10^3
NH_3^+	4.4‡	1.6×10^4	2.4	6.7×10^3		–	–	–
	4.7‡	7.7×10^4	12	6.4×10^3				
NH_2	7.5	2.3×10^5	64	3.6×10^3		-	-	-

*Rate constants $(k_c/K_m)^G$ and k_c^G were determined with substrates containing oxygen or sulfur at the *pro*-S_P position of the reactive phosphoryl group (P–O and P–S, respectively; Table 1, I–III and IX–XI) in side-by-side experiments under conditions such that the chemical step is rate limiting, as described in the Materials and methods section, and were measured at 10 mM Mg^{2+} unless otherwise specified. Each rate constant represents the average of at least two independent determinations that vary by < 20%. Addition of up to 1 mM DTT or EDTA had no significant effect on the observed rate constants (< 20%). –, not determined. †2′-X refers to the 2′-substituent at U(–1). ‡Determined at 100 mM Mg^{2+}. §The thio effect is 4–5-fold larger for $(k_c/K_m)^G$ than for k_c^G. This is presumably because the P–O and P–S containing substrates bind the ribozyme in different conformations. The ribozyme binds oligonucleotide substrates in two steps: formation of an open complex, in which S is held solely by base-pairing interactions with the internal guide sequence of E to form the P1 duplex, followed by docking of P1 into the ribozyme core via tertiary interactions to form the closed complex ([59–61] and references therein). The P–O-containing substrates bind the ribozyme to form closed complexes, whereas the P–S-containing substrates bind the ribozyme to form open complexes (data not shown). The guanosine nucleophile binds ~fivefold more strongly to the closed complex than to the open complex [58]. Thus, binding of G to the E•S complexes formed by the P–O-containing substrates is expected to be ~fivefold stronger than those formed by the P–S-containing substrates. This has been verified for several substrates (data not shown).

were followed [$(k_c/K_m)^G$ and k_c^G, respectively; Table 2]. Thio substitution of the *pro-*S_P oxygen (P–O → P–S) has a similar effect on the rate constants of each substrate, regardless of whether a 2′-OH, 2′-H, 2′-NH_3^+ or 2′-NH_2 is present at U(–1) (Table 3). The observed thio effects are independent of pH and Mg^{2+} concentration (Table 3). The constant thio effect observed with different 2′-substituents at U(–1) suggests that the catalytic contribution of the 2′-substituent at U(–1) is independent of the presence of sulfur or oxygen at the *pro-*S_P position of the reactive phosphoryl group. There is therefore no indication of a direct hydrogen bond between the 2′-OH and the *pro-*S_P oxygen.

Finally, we probed the hydrogen bond between the 2′-OH and the 3′-oxygen of U(–1) (Figure 1b) by replacing this 3′-oxygen with sulfur. The rate of the reaction E•S•G → products (k_c^G) was determined for 3′-thio substituted substrates with either 2′-OH or 2′-H at U(–1) [$rS_{OH,3'-S}$ and $rS_{H,3'-S}$, respectively (Table 1)]. In the presence of 10 mM Mg^{2+}, the rate constant of the chemical step for the thio-substituted substrates is similar with 2′-OH or 2′-H at the cleavage site (within twofold; Table 4). The experiment was repeated with added Mn^{2+}, as the presence of 3′-bridging sulfur severely compromises reactivity in Mg^{2+} alone, whereas reaction of 3′-thio substituted substrates can be rescued by replacing the Mg^{2+} at site A with Mn^{2+} (Figure 1b, M_A; [11] and data not shown). Mn^{2+} binds to metal site A with an apparent dissociation constant of $K^{Mn,app}$ = 0.8 mM (10 mM Mg^{2+}; [13]), so that 10 mM Mn^{2+} allows Mn^{2+} to fully replace Mg^{2+} at site A. With metal site A occupied by Mn^{2+}, rate constants for reaction of 3′-thio-substituted substrates are similar with 2′-OH or 2′-H at U(–1) (Table 4). Thus, the 2′-OH at U(–1) does not make a significant contribution to the chemical step with substrates containing a 3′-sulfur leaving group, whether Mg^{2+} or Mn^{2+} is bound at metal site A. This is in marked contrast to the 10^3-fold faster reaction with 2′-OH than 2′-H for substrates with an oxygen at the 3′-bridging position (Table 3) [2]. The removal of the catalytic advantage of the 2′-OH of U(–1) by the 3′-thio substitution is most simply interpreted in terms of a direct hydrogen bond between the 2′-OH and the 3′-bridging oxygen (Figure 1b).

In summary, the results presented in this section provide no indication of a hydrogen bond between the 2′-OH of U(–1) and the nonbridging oxygens of the reactive phosphoryl group (Figure 1c). In contrast, the results provide experimental support for the catalytic model previously proposed, in which the 2′-OH of U(–1) donates a hydrogen bond to one of the lone-pair electrons on the 3′-bridging oxygen in the transition state (Figures 1b and 4) [2,4,6]. The 3′-leaving group oxygen is partially anionic in the transition state, favoring formation of such a hydrogen bond; in contrast, this oxygen is electron-deficient in the ground state, rendering this hydrogen-bonding interaction less favorable [2,43,44]. Donation of a hydrogen bond from the neighboring 2′-OH to the 3′-bridging oxygen presumably provides a specific stabilization of the transition state relative to the ground state, thereby facilitating the chemical step. The developing negative charge on the leaving oxygen atom is apparently further stabilized by a metal ion, which interacts with the other lone pair of electrons on this oxygen (Figures 1b and 4, M_A; [11]; A.Y. *et al.*, unpublished observations). It appears that the *Tetrahymena* ribozyme focuses many of its active-site interactions on this 3′-leaving-group oxygen to provide rate acceleration. This is sensible as this atom presumably undergoes the largest amount of charge rearrangement in the course of the reaction.

Alignment of the 2′-OH by the ribozyme active site?

Although the 2′-OH of U(–1) appears to stabilize the developing negative charge on the 3′-bridging oxygen in the *Tetrahymena* ribozyme reaction, the 2′-OH has only a modest effect on the pK_a value of the 3′-OH group in aqueous solution (the pK_a values of the 3′-OH of ribose and 2′-deoxyribose are 12.1 and 12.6, respectively [45,46]). This

Table 4

Contribution of the 2′-OH at U(–1), relative to 2′-H, on the rate of the chemical step (k_c^G) with a 3′-sulfur or 3′-oxygen leaving group.*

M_A†	3′-O			3′-S		
	k_c^G (min^{-1})		k^{rel}‡	k_c^G (min^{-1})		k^{rel}‡
	2′-OH	2′-H		2′-OH	2′-H	
Mg^{2+}	0.84	9.7×10^{-4}	870	2.5×10^{-5}	1.4×10^{-5}	1.8
Mn^{2+}	–	–	–	7.0×10^{-2}	7.8×10^{-2}	0.9

*The rate constant k_c^G was determined with oligonucleotide substrates containing oxygen or sulfur at the 3′-leaving group (3′-O and 3′-S, respectively; Table 1, I–II and VII–VIII) in side-by-side experiments under conditions such that the chemical step is rate-limiting, as described in the Materials and methods section. The rate constants reported for substrates with 3′-O were determined at pH 5.2, and those with 3′-S were determined at pH 7.0. Varying the pH from 5.0 to 8.1 did not significantly change the k^{rel} values for the 3′-S containing substrate (10 mM Mn^{2+} / 10 mM Mg^{2+}; data not shown). †M_A refers to the metal ion (Mg^{2+} or Mn^{2+}) bound at metal site A (Figure 1, M_A). Values of k_c^G with Mg^{2+} bound at site A were determined at 10 mM Mg^{2+}, and those with Mn^{2+} bound were determined at 10 mM Mn^{2+} / 10 mM Mg^{2+} (see text). ‡$k^{rel} = (k_c^G,2'\text{-OH})/(k_c^G,2'\text{-H})$ is the rate constant for reaction of the substrate with 2′-OH at U(–1) relative to that with 2′-H.

suggests that the 2′-OH does not significantly stabilize the adjacent 3′-oxyanion in aqueous solution. Why, then, is the ribozyme reaction 10^3-fold faster with a 2′-OH than a 2′-H at U(–1)? As described in the Introduction section, the catalytic contribution of the 2′-OH of U(–1) is reduced upon mutating the G•U wobble pair or upon modifying the 2′-OH of A207 [4,6]. These results, in conjunction with crystallographic observations (see the Introduction section) [18,19], suggest a network of interactions surrounding the 2′-OH of U(–1) within the ribozyme active site that is not present in aqueous solution. As proposed previously [6], the 2′-OH of A207 may donate a hydrogen bond to the 2′-OH of U(–1) and bridge between this 2′-OH and the exocyclic amine of the G•U wobble pair (Figure 4).

Figure 4

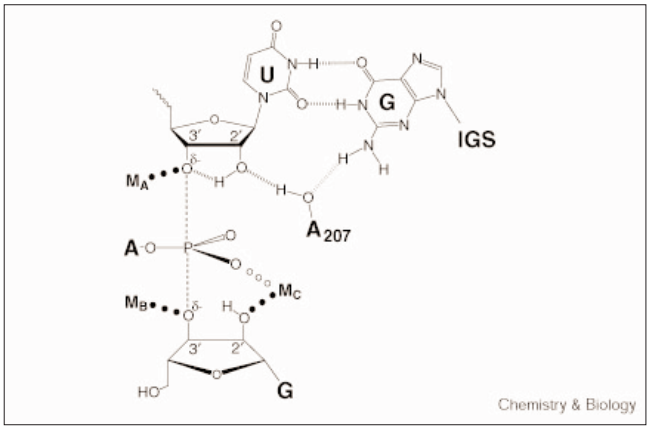

Model of transition state interactions within the *Tetrahymena* ribozyme active site. The dashed lines (---) depict the partial bond from the reactive phosphorus to the 3′-OH of G and the 3′-oxygen of the U(–1) residue of S, and 'δ-' depict the partial negative charges on the 3′-oxygens of U(–1) and G, as described in Figure 1. M_A, M_B and M_C are the three active-site metal ions that interact with the 3′-bridging oxygen of U (–1) and the 3′- and 2′-OH of G, as described in the legend to Figure 1 [7,10–12]. The results described here provide experimental evidence for a hydrogen bond from the 2′-OH of U(–1) to the 3′-bridging oxygen, as was previously proposed [2]. Previous work suggests that this 2′-OH may also participate in a hydrogen-bonding network that involves the 2′-OH of A207 and the G•U wobble pair that precedes the cleavage site [4,6,18].

Nevertheless, it is difficult to ascribe catalytic contributions to individual active-site groups; the difficulty is more pronounced for the groups discussed here as they are interconnected to form a network. Two extreme models can be presented that are both consistent with the previous data. As suggested previously, interactions with A207 and the G•U pair may be used to orient the 2′-hydroxyl proton of U(–1), thereby favoring formation of the hydrogen bond to the 3′-oxygen in the ribozyme reaction [4,6]. Alternatively, the network of interactions surrounding the 2′-OH may limit rearrangement within the active site relative to aqueous solution, such that replacing the 2′-OH by 2′-H is particularly deleterious for the ribozyme reaction. That is, in aqueous solution, the hydroxyl groups from water can stabilize the 3′-oxyanion when the 2′-OH is removed, such that this modification has no significant effect on the pK_a value of the 3′-OH. In contrast, in the ribozyme active site, access to water may be limited because the pocket created by removal of the 2′-OH may not be sufficient to readily accommodate a water molecule and because there would be a substantial energetic penalty for rearranging the active-site network surrounding the 2′-OH.

The network of interactions between the 2′-OH of U(–1), the 2′-OH of A207 and the exocyclic amine of G22 have been referred to as a 'catalytic triad' [6]. The energetic behavior of this network appears to be distinct, however, from the highly cooperative interactions found within the catalytic triad of serine proteases, in which mutation of any of the sidechains essentially removes the catalytic contribution of other groups within the triad [47]. In contrast, although an energetic interaction between the 2′-OH of U(–1) and the G•U wobble pair was suggested from the fivefold reduction in the contribution of the 2′-OH upon changing the G•U wobble to a G•C pair (Figure 4) [4], a catalytic contribution of 10^2-fold from this 2′-OH (relative to 2′-H) remains even with a G•C pair at the cleavage site. Furthermore, after removal of the exocyclic amine of G22, the effect of removing the 2′-OH of U(–1) remains within twofold of that of the wild-type ribozyme [5], and replacing the 2′-OH of A207 with 2′-H or 2′-F still has a deleterious effect on ribozyme function [6]. These observations suggest that the exocyclic amine of G22 is not required for the 2′-OH of U(–1) or the 2′-OH of A207 to make its interactions. In addition, these energetic effects suggest the presence of a more extensive network of interactions within this RNA active site that restricts positioning even in the absence of the exocyclic amine of G22. In contrast, the observation that the chemical step for $rSNH_3^+$ is faster than rS_{OH} (Figure 2 and equation 2), despite the absence of lone-pair electrons on the 2′-NH_3^+ group to accept a hydrogen bond from A207, suggests that there is some ability to rearrange active-site groups within this network. It will be fascinating to explore further the energetic behavior of this active-site network within the *Tetrahymena* ribozyme, to unravel the structural basis for its behavior, and to compare its behavior with those of other RNA and protein enzymes.

Catalytic role of the cleavage site 2′-OH in other RNA enzymes

The 2′-OH at the cleavage site of group II introns makes only a small contribution to catalysis; replacing this 2′-OH by 2′-H reduces the observed reaction rate by less than 30-fold [48]. This suggests that the cleavage site 2′-OH is not used by group II introns for catalysis. The ability of group II introns to utilize DNA substrates could facilitate their integration into new genomic positions and is presumably important for the mobility of some group II introns

(e.g. [49–52] and references therein). The small effect of removing the cleavage site 2′-OH in group II introns contrasts with the 10^3-fold effect observed in the *Tetrahymena* group I ribozyme, and provides further support for the presence of a network of active-site interactions within the *Tetrahymena* RNA active site that accentuates the energetic cost for removal of this 2′-OH.

Large catalytic contributions of the 2′-OH preceding the scissile bond have also been observed with several other RNA enzymes that carry out reactions similar to that catalyzed by the *Tetrahymena* group I ribozyme. Replacing the 2′-OH by a 2′-H results in a ~2000-fold reduction in reaction rate for the *Anabaena* group I ribozyme [53], and a 3400-fold rate reduction for the RNA component of RNase P [9]. Mechanistic models such as stabilization of the neighboring 3′-leaving-group oxygen and stabilization of bound active-site metal ion(s) have been proposed (e.g. [9]) but remain to be tested. Experiments analogous to those described here might be useful in delineating the catalytic role of the cleavage site 2′-OH groups in these ribozyme reactions.

Significance

The discovery of RNA catalysis has generated much biochemical and mechanistic interest. Delineating the catalytic interactions utilized by an RNA enzyme and dissecting the properties of its active site are central to understanding how RNA enzymes are able to act as efficient biological catalysts. In this work, site-specific substrate modifications combined with quantitative analysis have been used to test several catalytic models proposed for the 2′-OH of U(–1) in the *Tetrahymena* group I ribozyme reaction. The results provide experimental support for a previously proposed model in which the 2′-OH donates a hydrogen bond to the neighboring 3′-bridging oxygen, thereby stabilizing the developing negative charge on the leaving group oxygen in the transition state. These results demonstrate the utility of chemical modification combined with in-depth mechanistic analysis as a tool for delineating the catalytic roles of individual active-site groups. Analogous approaches can be used to dissect catalytic interactions in the active sites of other RNA and protein enzymes (e.g. [54]).

The large deleterious effect of removing the 2′-OH of U(–1) suggests that this 2′-OH is situated within a network of active-site interactions. A model has been proposed in which the 2′-OH of U(–1), the 2′-OH of A207 and the exocylic amine of G22 forms a hydrogen-bonding network. Nevertheless, the energetic behavior of this network is complex, suggesting that the contribution of the individual groups within this network cannot be simply dissected. The presence of additional functional groups involved and the structural bases for the energetic behavior of this network remain important questions for future investigations.

Materials and methods

Materials

Ribozyme was prepared by *in vitro* transcription with T7 RNA polymerase as described previously [55]. Oligonucleotides were made by solid-phase synthesis and supplied by the Protein and Nucleic Acid Facility at Stanford University or were gifts from L. Beigelman (Ribozyme Pharmaceuticals Inc.) or F. Eckstein. Oligonucleotides containing a bridging sulfur at the 3′-moiety of U(–1) were synthesized by published procedures [56]. Oligonucleotide substrates were 5′-end-labeled using [γ-^{32}P]ATP and T4 polynucleotide kinase and purified by electrophoresis on 24% nondenaturing polyacrylamide gels, as described previously [31,55].

General kinetic methods

All reactions were single turnover, with ribozyme in excess of labeled oligonucleotide substrate (S*) and were carried out at 30°C in 50 mM buffer. The buffers used were: sodium acetate, pH 4.4–5.6; NaMES, pH 5.4–7.0, NaMOPS, pH 6.4–7.1, NaHEPES, 6.8–7.5, NaEPPS, pH 7.5–8.5 (pH values determined at 30°C). Reactions were followed and analyzed essentially as described previously [57,58]. Briefly, ribozyme was preincubated in 10 mM $MgCl_2$ and 50 mM buffer at 50°C, cooled to 30°C, and Mg^{2+}, Mn^{2+}, Zn^{2+}, Cd^{2+} or Co^{2+} was added to obtain the desired metal ion concentrations prior to initiating the reaction by addition of S* (< 0.1 nM). For reactions with 0.1 mM Mg^{2+} background, ribozyme was folded in 2 mM $MgCl_2$ at 50°C, cooled to 30°C, and adjusted to desired metal ion concentrations. For reactions carried out above pH 8.0, the preincubation was carried out at pH 7.5 to avoid degradation and diluted tenfold into the appropriate buffer at 30°C [21]. Six aliquots of 2 µl reaction mixture were removed from 20 µl reactions at specified times, and further reaction was quenched by addition of 4 µl of stop solution [90% formamide with EDTA in ≥ twofold excess of total divalent metal ion (20–200 mM), 0.005% xylene cyanole, 0.01% bromophenol blue and 1 mM Tris, pH 7.5]. Oligonucleotide substrates and products were separated by electrophoresis on 20% polyacrylamide/7 M urea gels, and their ratio at each time point was quantitated with a Molecular Dynamics Phosphorimager.

Reactions were followed for $\geq 3t_{1/2}$ except for very slow reactions. Good first-order fits to the data, with endpoints of ≥ 90%, were obtained (KaleidaGraph). The slow reactions were typically linear for up to 20 h, and an endpoint of 95% was assumed to obtain observed rate constants from the initial rates.

Kinetic constants

The nomenclature used for rate constants is defined in Table 2. k_c^G, the first-order rate constant, was determined for oligonucleotide substrates I, II and VII–X (Table 1) with E saturating with respect to S (50–1000 nM E; $K_d^S \leq 8$ nM; data not shown) and with saturating G (2 mM; $K_d^G \leq 500$ µM). The second-order rate constant $(k_c/K_m)^G$ was determined for oligonucleotide substrates I–III and IX–XI (Table 1) with E saturating with respect to S as above, but with G subsaturating (≥ three concentrations, each > fivefold below K_d^G). The second-order rate constant $(k_c/K_m)^S$ was determined for oligonucleotide substrates IV–VI (Table 1) with saturating G (2 mM) but with E subsaturating with respect to S (10–50 nM E; $K_d^S \geq 150$ nM; data not shown).

Following the chemical step for reaction of dS_{NH_2}

To determine the effect of metal ions on the reactivity of dS_{NH_2}, it is crucial that the chemical step is rate limiting and that the reaction of deprotonated dS_{NH_2}, rather than $dS_{NH_3^+}$, was followed. The following suggest that the chemical step is rate limiting for the reaction: E•G + dS_N → products over the range of pH (4.4–7.9) and metal ion concentrations investigated; there is a constant thio-effect of 2.1 ± 0.2-fold at the *pro*-R_P oxygen (see text; data not shown); $(k_c/K_m)^S$ for dS_N is at least fivefold slower than for dS_{OH} under all the conditions tested (Figure 3a and data not shown); $(k_c/K_m)^S$ for dS_N is log-linear with pH and parallels the pH dependence of dS_H (10 mM Mg^{2+}, 10 mM Mn^{2+} / 0.1 mM Mg^{2+} and 10 mM Mn^{2+} / 2 mM Mg^{2+}; data not shown). The observation that the pH dependence of $(k_c/K_m)^S$ for dS_N parallels that for dS_H further suggests that deprotonation of the 2′-NH_3^+ group to

give dS_{NH_2} does not affect the rate constant of the reaction: E•G + S → products. If dS_{NH_2} were substantially less reactive than $dS_{NH_3^+}$, $(k_c/K_m)^S$ for dS_N would be expected to level off as the 2′-NH_3^+ group deprotonates above pH 6 [20,26], analogous to the leveling-off of the rate constant for the reaction: E•rS_N + G → products (Figure 2). The absence of a rate effect from deprotonation of the 2′-group in the reaction: E•G + S → products, despite the faster rate of the chemical step from the E•S complex for substrates with 2-NH_3^+ than with 2′-NH_2 at U(–1) (Figure 2), is presumably due to the weaker binding of substrates with 2-NH_3^+ than 2′-NH_2 at U(–1). Compared to 2′-OH or 2′-NH_2, the 2′-NH_3^+ group weakens the stability of the P1 duplex formed between S and the internal guide sequence of E by at least 30-fold ([20,28] and S.S. & D.H., unpublished results). Thus, the reaction of dS_{NH_2} can be followed at pH 7.5, without significant contribution from reaction of the small fraction of $dS_{NH_3^+}$ present at this pH (0.05; pK_a ~6.2 [20]).

Determination of the pK_a of the 2′-NH_3^+ group in the E•rS_N complex

The different reactivities of $rS_{NH_3^+}$ in the reaction: E•S + G → products $[(k_c / K_m)^G]$ provide a signal for deprotonation of the -NH_3^+ group in the E•rS_N complex (Figure 2). The value of $pK_a^{E•rS_N}$, the negative logarithm of the observed equilibrium constant for deprotonation of the -NH_3^+ group in E•rS_N, was obtained from the pH dependence of $(k_c / K_m)^G$ for rS_N relative to rS_{OH}, $(k_c / K_m)^{G,rel}$. The data were fit to equation 3, which was derived from equation 2:

$$(k_c/K_m)^{G,rel}_{obsd} = (k_c/K_m)^{G,rel}_{rSNH_2} \times \frac{K_a^{E•rS_N}}{K_a^{E•rS_N} + [H^+]} + (k_c/K_m)^{G,rel}_{rSNH_3^+} \times \frac{[H^+]}{K_a^{E•rS_N} + [H^+]} \quad (3)$$

$(k_c / K_m)^{G,rel}_{obsd}$ is the observed second-order rate constant for reaction of rS_N relative to rS_{OH} at a particular pH, and $(k_c / K_m)^{G,Rel}_{rSNH_3^+}$ and $(k_c / K_m)^{G,rel}_{rSNH_2}$ are the pH-independent rate constants for reaction of $rSNH_3^+$ and $rSNH_2$, respectively, relative to rS_{OH}. The pK_a of 5.0 obtained for the 2′-amino group in E•rS_N is lower than the solution pK_a of this group of 6.2 [20]. This is presumably due to the ~30-fold weaker affinity of the oligonucleotide substrate with 2′-NH_3^+ than with 2′-NH_2 at U(–1) (see previous section), as illustrated in the thermodynamic cycle of equation 4:

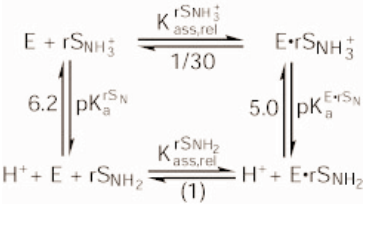

(4)

In equation 4, the affinities of $rSNH_3^+$ and $rSNH_2$ are expressed as equilibrium association constants relative to rS_{OH} ($K_{ass,rel}$) in order to correct for a small pH effect on substrate affinity that is not specific to the 2′-amino group (2–3-fold). The thermodynamic relationship in equation 4 predicts that the equilibrium for deprotonation of the 2-NH_3^+ group (K_a) would be 30-fold more favorable on the ribozyme than in aqueous solution:

$$\frac{K_a^{E•rS_N}}{K_a^{rS_N}} = \frac{K_{ass,rel}^{rSNH_2}}{K_{ass,rel}^{rSNH_3^+}} = 30; \quad (5)$$

$pK_a^{E•rSN} = pK_a^{rSN} - \log 30 = 6.2 - 1.47 = 4.7$. The predicted pK_a of 4.7 for the U(–1) 2′-amino group in the E•rS_N complex is the same, within error, as the value of $pK_a^{E•rS_N} = 5.0$ determined experimentally (Figure 2).

Acknowledgements

We are grateful to L. Beigelman and F. Eckstein for the gift of oligonucleotide substrates, G. Narlikar for initial results and intellectual input, and members of the Herschlag lab for comments on the manuscript. This work was supported by grants from NIH to D.H. and HHMI to J.A.P.

References

1. Cech, T.R. & Herschlag, D. (1996). Group I ribozymes: substrate recognition, catalytic strategies, and comparative mechanistic analysis. In *Nucleic Acids and Molecular Biology.* (Eckstein, F. & Lilley, D.M.J., eds), pp. 1-17, Springer-Verlag, Berlin.
2. Herschlag, D., Eckstein, F. & Cech, T.R. (1993). The importance of being ribose at the cleavage site in the *Tetrahymena* ribozyme reaction. *Biochemistry* **32**, 8312-8321.
3. Sugimoto, N., Tomka, M., Kierzek, R., Bevilacqua, R.C. & Turner, D.H. (1989). Effects of substrate structure on the kinetics of circle opening reactions of the self-splicing intervening sequence from *Tetrahymena thermophila*: evidence for substrate and Mg^{2+} binding interactions. *Nucleic Acids Res.* **17**, 355-371.
4. Knitt, D.S., Narlikar, G.J. & Herschlag, D. (1994). Dissection of the role of the conserved G•U pair in group I RNA self-splicing. *Biochemistry* **33**, 13864-13879.
5. Strobel, S.A. & Cech, T.R. (1996). Exocyclic amine of the conserved G•U pair at the cleavage site of the *Tetrahymena* ribozyme contributes to 5′-splice site selection and transition state stabilization. *Biochemistry* **35**, 1201-1211.
6. Strobel, S.A. & Ortoleva-Donnelly, L. (1999). A hydrogen-bonding triad stabilizes the chemical transition state of a group I ribozyme. *Chem. Biol.* **6**, 153-165.
7. Sjögren, A.-S., Pettersson, E., Sjöberg, B.-M. & Strömberg, R. (1997). Metal ion interaction with cosubstrate in self-splicing of group I introns. *Nucleic Acids Res.* **25**, 648-653.
8. Sugimoto, N., Kierzek, R. & Turner, D.H. (1988). Kinetics for reaction of a circularized intervening sequence with CU, UCU, CUCU and CUCUCU: mechanistic implications from the dependence on temperature and on oligomer and Mg^{2+} concentrations. *Biochemistry* **27**, 6384-6392.
9. Smith, D. & Pace, N.R. (1993). Multiple magnesium ions in the ribonuclease P reaction mechanism. *Biochemistry* **32**, 5273-5281.
10. Shan, S. & Herschlag, D. (1999). Probing the role of metal ions in RNA catalysis: kinetic and thermodynamic characterization of a metal ion interaction with the 2′-moiety of the guanosine nucleophile in the *Tetrahymena* ribozyme reaction. *Biochemistry* **38**, 10958-10975.
11. Piccirilli, J.A., Vyle, J.S., Caruthers, M.H. & Cech, T.R. (1993). Metal-ion catalysis in the *Tetrahymena* ribozyme reaction. *Nature* **361**, 85-88.
12. Weinstein, L.B., Jones, B.C., Cosstick, R. & Cech, T.R. (1997). A second catalytic metal ion in a group I ribozyme. *Nature* **388**, 805-808.
13. Shan, S., Yoshida, A., Sun, S., Piccirilli, J. & Herschlag, D. (1999). Three distinct metal ions at the active site of the *Tetrahymena* group I ribozyme. *Proc. Natl Acad. Sci. USA* **96**, 12299-12304.
14. Yoshida, A., Sun, S. & Piccirilli, J. A. (1999). A new metal ion interaction in the *Tetrahymena* ribozyme reaction revealed by double sulfur substitution. *Nat. Struct. Biol.* **6**, 318-321.
15. Benkovic, S.J. & Schray, K.J. (1973). Chemical basis of biological phosphoryl transfer. In *The Enzymes.* (Boyer, P.P., ed.), pp. 201-238, Academic Press, New York.
16. Cooperman, B.S. (1976). The role of divalent metal ions in phosphoryl and nucleotidyl transfer. In *Metal Ions in Biological Systems.* (Sigel, H., ed.), pp. 79-125, Marcel Dekker, New York.
17. Admiraal, S. & Herschlag, D. (1995). Mapping the transition-state for ATP hydrolysis: Implications for enzymatic catalysis. *Chem. Biol.* **2**, 729-739.
18. Holbrook, S. R., Cheong, C., Tinoco, I. & Kim, S.-H. (1991). Crystal structure of an RNA double helix incorporating a track of non-watson-crick base pairs. *Nature* **353**, 579-581.
19. Mueller, U., Schubel, H., Sprinzl, M. & Heinemann, U. (1999). Crystal structure of acceptor stem of $tRNA^{Ala}$ from *Escherichia coli* shows unique G•U wobble base pair at 1.16° resolution. *RNA* **5**, 670-677.
20. Aurup, H., Tuschl, T., Benseler, F., Ludwig, J. & Eckstein, F. (1994). Oligonucleotide duplexes containing 2′-amino-2′-deoxycytidines: thermal stability and chemical reactivity. *Nucleic Acids Res.* **22**, 20-24.
21. Knitt, D.S. & Herschlag, D. (1996). pH Dependencies of the *Tetrahymena* ribozyme reveal an unconventional origin of an apparent pK_a. *Biochemistry* **35**, 1560-1570.
22. Celander, D.W. & Cech, T.R. (1991). Visualizing the higher order folding of a catalytic RNA molecule. *Science* **251**, 401-407.
23. Latham, J.A. & Cech, T.R. (1989). Defining the inside and outside of a catalytic RNA molecule. *Science* **245**, 276-282.
24. Wang, J.F. & Cech, T.R (1994). Metal ion dependence of active-site structure of the *Tetrahymena* ribozyme revealed by site-specific photo-cross-linking. *J. Am. Chem. Soc.* **116**, 4178-4182.

25. Herschlag, D. & Khosla, M. (1994). Comparison of pH dependencies of the *Tetrahymena* ribozyme reactions with RNA 2′-substituted and phosphorothioate substrates reveals a rate-limiting conformational step. *Biochemistry* **33**, 5291-5297.
26. Shan, S., Narlikar, G.N. & Herschlag, D. (1999). Protonated 2′-aminoguanosine as a probe of the electrostatic environment of the active site of the *Tetrahymena* group I ribozyme. *Biochemistry* **38**, 10976-10988.
27. Herschlag, D., Piccirilli, J.A. & Cech, T.R. (1991). Ribozyme-catalyzed and nonenzymatic reactions of phosphate diesters: rate effects upon substitution of sulfur for a nonbridging phosphoryl oxygen atom. *Biochemistry* 30, 4844-4854.
28. Narlikar, G.J., Khosla, M., Usman, N. & Herschlag, D. (1997). Quantitating tertiary binding energies of 2′OH groups on the P1 duplex of the *Tetrahymena* ribozyme: Intrinsic binding energy in an RNA enzyme. *Biochemistry* **36**, 2465-2477.
29. Sille'n, L.G. & Martell, A.E. (1964). *Stability Constants of Metal-Ligand Complexes, Special publicaton 17*. The Chemical Society, London.
30. Martell, A.E. & Smith, R.M. (1976). *Critical Stability Constants.* Plenum, New York.
31. Herschlag, D., Eckstein, F. & Cech, T.R. (1993). Contribution of 2′-hydroxyl groups of the RNA substrate to binding and catalysis by the Tetrahymena ribozyme. An energetic picture of an active site composed of RNA. *Biochemistry* **32**, 8299-8311.
32. Schreier, A.A. & Schimmel, P.R. (1974). Interaction of manganese with fragments, complementary fragment recombinations, and whole molecules of yeast phenylalanine specific transfer RNA. *J. Mol. Biol.* **86**, 601-620.
33. Ott, G., Arnold, L. & Limmer, S. (1993). Proton NMR studies of manganese ion binding to tRNA-derived acceptor arm duplexes. *Nucleic Acids Res.* **21**, 5859-5864.
34. Walter, F., Murchie, A.I.H., Thomson, J.B. & Lilley, D.M.J. (1998). Structure and activity of the hairpin ribozyme in its natural junction conformation: Effect of metal ions. *Biochemistry* **37**, 14195-14203.
35. Bass, B.L. & Cech, T.R. (1986). Ribozyme inhibitors: deoxyguanosine and dideoxyguanosine are competitive inhibitors of self-splicing of the *Tetrahymena* ribosomal ribonucleic acid precursor. *Biochemistry* **25**, 4473-4477.
36. Tanner, N.K. & Cech, T.R. (1987). Guanosine binding required for cyclization of the self-splicing intervening sequence ribonucleic acid from *Tetrahymena thermophila*. *Biochemistry* **26**, 3330-3340.
37. Crampton, M.R. (1974). Acidity and hydrogen bonding. In *Chemistry of the Thiol Group.* (Patai, S., ed.), pp 379-415, John Wiley & Sons, New York.
38. Abboud, J.-L.M. & Taft, R.W. (1988). Studies on amphiprotic compounds. 3. Hydrogen-bonding basicity of oxygen and sulfur compounds. *J. Org. Chem.* **53**, 1545-1550.
39. Meot-Ner, M. & Sieck, L.W. (1986). The ionic hydrogen bond and ion solvation. 5. OH•••O$^-$ bonds. Gas-phase solvation and clustering of alkoxide and carboxylate anions. *J. Am. Chem. Soc.* **108**, 7525-7529.
40. Sieck. L.W. & Meot-Ner, M. (1989). Ionic hydrogen bond and ion solvation. 8. RS$^-$•••HOR bond strengths. Correlation with acidities. *J. Phys. Chem.* **93**, 1586-1588.
41. Allen, F.H., Bird, C.M., Rowland, R.S. & Raithby, P.R. (1997). Hydrogen-bond acceptor and donor properties of divalent sulfur (Y-S-Z and R-S-H). *Acta Crystallogr. B* **53**, 696-701.
42. Platts, J.A., Howard, S.T. & Bracke, B.R.F. (1996). Directionality of hydrogen bonds to sulfur and oxygen. *J. Am. Chem. Soc.* **118**, 2726-2733.
43. Williams, A. (1992). Effective charge and transition-state structure in solution. *Adv. Phys. Org. Chem.* **27**, 1-55.
44. Narlikar, G.J., Gopalakrishnan, V., McConnel, T.S., Usman, N. & Herschlag, D. (1995). Use of binding energy by an RNA enzyme for catalysis by positioning and substrate destabilization. *Proc. Natl Acad. Sci. USA* **92**, 3668-3672.
45. Christensen, J.J., Rytting, J.H. & Izatt, R.M. (1970). Thermodynamics of proton dissociation in dilute aqueous solution. Part XV. Proton dissociation from several monosaccharides at 10 and 40°C. *J. Chem. Soc. B*, 1646-1648.
46. Izatt, R.M., Rytting, J.H., Hansen, L.D. & Christensen, J.J. (1966). Thermodynamics of proton dissociation in dilute aqueous solution. V. An entropy titration study of adenosine, pentoses, hexoses, and related compounds. *J. Am. Chem. Soc.* **88**, 2641-2645.
47. Carter, P. & Wells, J.A. (1988). Dissecting the catalytic triad of a serine protease. *Nature* **332**, 564-568.
48. Griffin Jr., E.A., Qin, Z., Michels Jr., W.J. & Pyle, A.M. (1995). Group II intron ribozyme that cleave DNA and RNA linkages with similar efficiency, and lack contacts with substrate 2′-hydroxyl groups. *Chem. Biol.* **2**, 761-770.
49. Lambowitz, A.M. & Belfort, M. (1993). Introns as mobile genetic elements. *Annu. Rev. Biochem.* **62**, 587-622.
50. Yang, J., Mohr, G., Perlman, P.S. & Lambowitz, A.M. (1998). Group II intron mobility in yeast mitochondria: target DNA-primed reverse transcription activity of al1 and reverse splicing into DNA transposition sites in vitro. *J. Mol. Biol.* **282**, 505-523.
51. Matsuura, M., & Lambowitz, A.M. (1997). A bacterial group II intron encoding reverse transcriptase, maturase, and DNA endonuclease activities: biochemical demonstration of maturase activity and insertion of new genetic information within the intron. *Genes Dev.* **11**, 2910-2924.
52. Eickbush, T.H. (1999). Mobile introns: retrohoming by complete reverse splicing. *Curr. Biol.* **9**, R11-R14.
53. Zaug, A.J., Davila-Aponte, J.A. & Cech, T.R. (1994). Catalysis of RNA cleavage by a ribozyme derived from the group I intron of *Anabaena* pre-tRNA^{Leu}. *Biochemistry* **33**, 14935-14947.
54. Hondal, R. J., Bruzik, K. S., Zhao Z. & Tsai, M. D. (1997). Mechanism of phosphatidylinosito-phospholipase C. 2. Reversal of a thio effect by site-directed mutagenesis. *J. Am. Chem. Soc.* **119**, 477-478.
55. Zaug, A.J., Grosshans, C.A. & Cech, T.R. (1988). Sequence-specific endoribonuclease activity of the *Tetrahymena* ribozyme: enhanced cleavage of certain oligonucleotide substrates that form mismatched ribozyme-substrate complexes. *Biochemistry* **27**, 8924-8931.
56. Sun, S., Yoshida, A. & Piccirilli, J. A. (1997). Synthesis of 3′-thioribonucleosides and their incorporation into oligoribonucleotides via phosphoramidite chemistry. *RNA* **3**, 1352-1363.
57. Herschlag, D. & Cech, T.R. (1990). Catalysis of RNA cleavage by the *Tetrahymena thermophila* ribozyme. 1. Kinetic description of the reaction of an RNA substrate complementary to the active site. *Biochemistry* **29**, 10159-10171.
58. McConnell, T.S., Cech, T.R. & Herschlag, D.H. (1993). Guanosine binding to the *Tetrahymena* ribozyme: thermodynamic coupling with oligonucleotide binding. *Proc. Natl Acad. Sci. USA* **90**, 8362-8366.
59. Herschlag, D. (1992). Evidence for processivity and two-step binding of the RNA substrate from studies of J1/2 mutants of the *Tetrahymena* ribozyme. *Biochemistry* **31**, 1386-1398.
60. Bevilacqua, P.C., Kierzek, R., Johnson, K.A. & Turner, D.H. (1992). Dynamics of ribozyme binding of substrate revealed by fluorescence-detected stopped-flow methods. *Science* **258**, 1355-1358.
61. Szewczak, A.A., Ortoleva-Donnelly, L., Ryder, S.P., Moncoeur, E. & Strobel, S.A. (1998). A minor groove RNA triple helix within the catalytic core of a group I intron. *Nat. Struct. Biol.* **5**, 1037-1042.

Because *Chemistry & Biology* operates a 'Continuous Publication System' for Research Papers, this paper has been published via the internet before being printed. The paper can be accessed from http://biomednet.com/cbiology/cmb – for further information, see the explanation on the contents pages.